Nanoscale Research Letters
a SpringerOpen Journal

NANO EXPRESS Open Access

Fabrication and spectroscopic investigation of branched silver nanowires and nanomeshworks

Xiao-Yang Zhang[1,2,3], Tong Zhang[1,2,3*], Sheng-Qing Zhu[1,2,3], Long-De Wang[1,2,3], Xuefeng Liu[4], Qi-Long Wang[1] and Yuan-Jun Song[1,2]

Abstract

Wide wavelength ranges of light localization and scattering characteristics can be attributed to shape-dependent longitude surface plasmon resonance in complicated nanostructures. We have studied this phenomenon by spectroscopic measurement and a three-dimensional numerical simulation, for the first time, on the high-density branched silver nanowires and nanomeshworks at room temperature. These nanostructures were fabricated with simple light-induced colloidal method. In the range from the visible to the near-infrared wavelengths, light has been found effectively trapped in those trapping sites which were randomly distributed at the corners, the branches, and the junctions of the nanostructures in those nanostructures in three dimensions. The broadened bandwidth electromagnetic field enhancement property makes these branched nanostructures useful in optical processing and photovoltaic applications.

Keywords: Silver Nanowires, Nanomeshworks, Branched nanostructures, Localized surface plasmon resonance, Hot spots, Bandwidth

Background

Noble metal nanostructures supporting surface plasmons arising from the coherent oscillations of the conduction electrons under the radiation of the incident light have been widely investigated [1-24]. The optical spectral signatures of the plasmonic nanostructures are mainly dependent on the distribution of the electromagnetic field on the surface of the metal nanostructures. When the size of the metal nanostructures is smaller than the wavelength of the incident light, they support localized surface plasmon resonance (LSPR) at particular resonance wavelengths [1]. The LSPR properties of the plasmonic nanostructures are size and shape dependent [1-3]. With the increase of the size of the metal nanostructures, high-order resonance occurs owing to the surface plasmon polariton (SPP) mode interferences. For example, metal nanowires support the Fabry-Perot (FP) modes [6], micron-size metal nanoplates support the whispering gallery modes [7], and the flag type of metal nanostructure supports competitive LSPR and FP modes simultaneously [23]. These metal nanostructures with regular shapes usually exhibit narrow-band resonance characteristic seen from their extinction spectra.

As well known, on the contrary to those elemental nanoparticles, metal nanostructures with complicated geometries, such as nanochains and branched nanowires assembled or fused by the elemental nanoparticles, show enhanced light-trapping ability [8-24]. When the metal nanoparticles are in close proximity or jointed together, the intensity of the localized electromagnetic field at the corner area and the junctions of these nanostructures are dramatically enhanced owing to the existing plasmon coupling between different propagation modes or resonance modes [8,9]. It is usually accompanied by obvious redshift and extension of their resonance bands [3,9]. The overall optical properties including obvious light-trapping and scattering enhancement in a wide wavelength range make these complicated metal nanostructures highly desirable in improving the performance of bio-chemical sensors [21,22], solar cells [24,25], and wide-bandwidth light-emitting diodes [26]. Although considerable progress has been made in the fabrication

* Correspondence: tzhang@seu.edu.cn
[1]School of Electronic Science and Engineering, Southeast University, Nanjing 210096, People's Republic of China
[2]Key Laboratory of Micro-Inertial Instrument and Advanced Navigation Technology, Ministry of Education, Nanjing 210096, People's Republic of China
Full list of author information is available at the end of the article

methods of such complicated metal nanostructures, such as laser welding [8-10], sintering triggered thermally [11] or chemically [12], electrodeposition [13], microwave irradiation [14], and chemical synthesis methods [15-22], it is still a challenge to fabricate high-yield metal nanostructures with excellent light-trapping property in a wide wavelength range to meet the practical demands for a large-scale production.

In this study, we present a simple and facile light-induced colloidal method to fabricate high-density branched silver nanowires and nanomeshworks. These complicated nanostructures showed significant light-trapping and scattering properties in the wide range from the visible to the near-infrared wavelengths, arising from the shape-dependent longitude surface plasmon resonance. The broadened bandwidth electromagnetic field enhancement characteristic makes these nanostructures useful in optical processing and photovoltaic applications.

Methods

The fabrication process of the branched silver nanowires and nanomeshworks includes two steps.

Synthesis of the silver seeds

The first step is the synthesis of the silver seeds. A 5-mL amount of 0.5 M trisodium citrate, 0.5 mL of 0.05 M L-arginine, 0.15 mL of 0.5 M polyvinylpyrolidone (PVP), and 0.2 mL of 0.5 M silver nitrite were added to 7 mL of deionized water while stirring slowly. Then, 2 mL of 0.4 M sodium borohydride ($NaBH_4$) was added to the solution slowly drop by drop. The color of the silver seed solution changed to dark brown rapidly.

Fabrication of the branched silver nanowires and nanomeshworks

The silver seed solution was stirred slowly for 20 min in a dark place. Then, it was exposed to a 400-W metal halide lamp covered by a blue glass filter (B-440 UV–vis bandpass filter, Edmund Optics Inc., Barrington, NJ, USA). The strategy of the light exposure procedure is shown in Figure 1a. A beaker containing silver seed solution was placed on the top surface of the glass filter. The top and the side wall of the beaker were covered by aluminum foils to avoid the influence of ambient light. The metal halide lamp was placed below the glass filter. The density of the light intensity passing through the glass filter is approximately 0.5 mW/cm^3. It can be varied by tuning the distance between the lamp and the glass filter. It is necessary to shake up the solution for several times to avoid the aggregation of the nanostructures during the exposure procedure. When the silver seeds were exposed to the blue light for approximately 5 h, high density branched nanostructure solution with black color were achieved. Considering H_2 as an outgrowth when $NaBH_4$ is used as a reducing agent in the reduction procedure, it is necessary to keep aeration when the solution with such a high material concentration is exposed to the light.

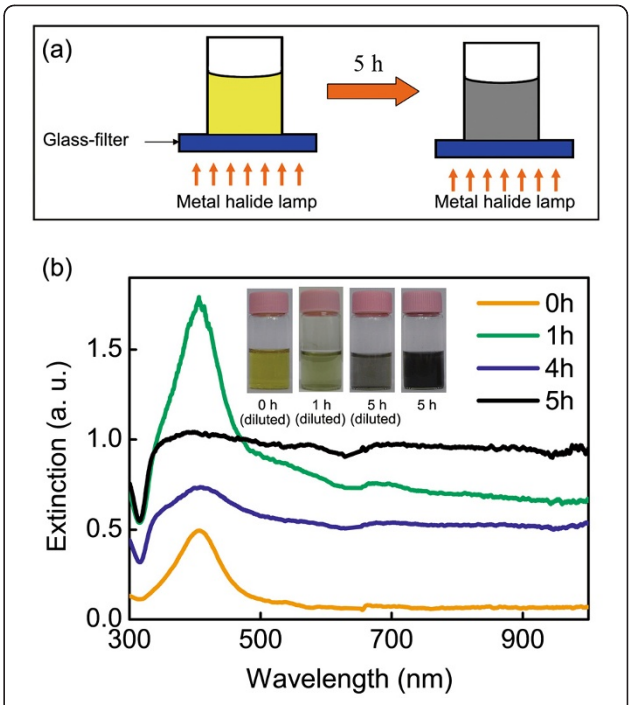

Figure 1 Scheme of the experiment and the optical characteristics of the silver solution. (**a**) The exposure process for the fabrication of branched silver nanowires and nanomeshworks. (**b**) The extinction spectra and the photographs of the silver nanostructure solutions at different exposure times.

Results and discussion

The color of conventional chemical synthesized silver nanowire solution is pale green accompanied with strong reflection [4] due to the narrow resonance bands and selective light localization properties. Figure 2 shows the typical LSPR spectrum of silver nanowire with smooth surface calculated by three-dimensional finite element method (FEM) [9,27,28]. The silver nanowire supports longitude SPP modes which reflect between its two terminal facets. Therefore, it shows periodic plasmon resonance bands with narrow bandwidth arising from the Fabry-Perot interference of the SPP modes. From the inset in Figure 2, one can see that the electric field is distributed at the surface and the ends of the nanowire. However, light localization and scattering enhancement mainly occur at the ends of the nanowire. Therefore, scattering is not obvious when the SPP modes are transmitted along the nanowires with smooth surface.

Compared with the conventional silver nanowire solution, silver solution prepared in our way containing branched nanostructures shows greatly enhanced light-trapping and

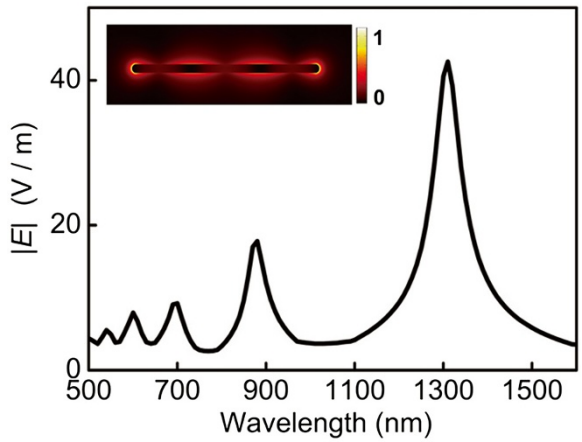

Figure 2 LSPR spectrum. Bare silver nanowire with a diameter of 30 nm and a length of 600 nm. The nanowire is surrounded by water (n = 1.33). The inset shows the normalized electric field distribution |E| at the center of the nanowire at a resonance wavelength λ = 1,320 nm.

scattering characteristics in a wide wavelength range. The two-step light-induced chimerical colloidal method used here was first reported by Pietrobon and Kitaev for the synthesis of decahedral silver nanoparticles [2]. The scheme of the light exposure process is shown in Figure 1a. Surprisingly, silver nanostructures with distinct morphology and optical spectral signatures were found when we increased the material concentration by 100 times higher. Figure 1b shows the extinction spectra of the silver solution measured by a fiber-optic spectrometer (PG2000, Ideaoptics Technology Ltd., Shanghai, China) and the photographs of the solution samples at different exposure times. The first step is the synthesis of the silver seed solution. As shown in the inset of Figure 1b, the color of the diluted silver seed solution (exposure time is 0 h) is light yellow. As shown in the extinction spectrum, a narrow resonance band at 420 nm corresponding to the LSPR wavelength of typical silver nanospheres with a diameter of several nanometers [3] can be observed. The second step is the light-induced regrowth process of the silver nanostructures which is highly dependent on the material concentration. At a low concentration as reported in [2], decahedral silver nanoparticles with uniform sizes and shapes are the ultimate product. However, when the material concentration was increased by 100 times, the ultimate products containing mainly the branched nanowires and nanomeshworks can be observed. As seen from the extinction spectra, the resonance band at 420 nm decreased, and the absorption ratio in the longer wavelength increased

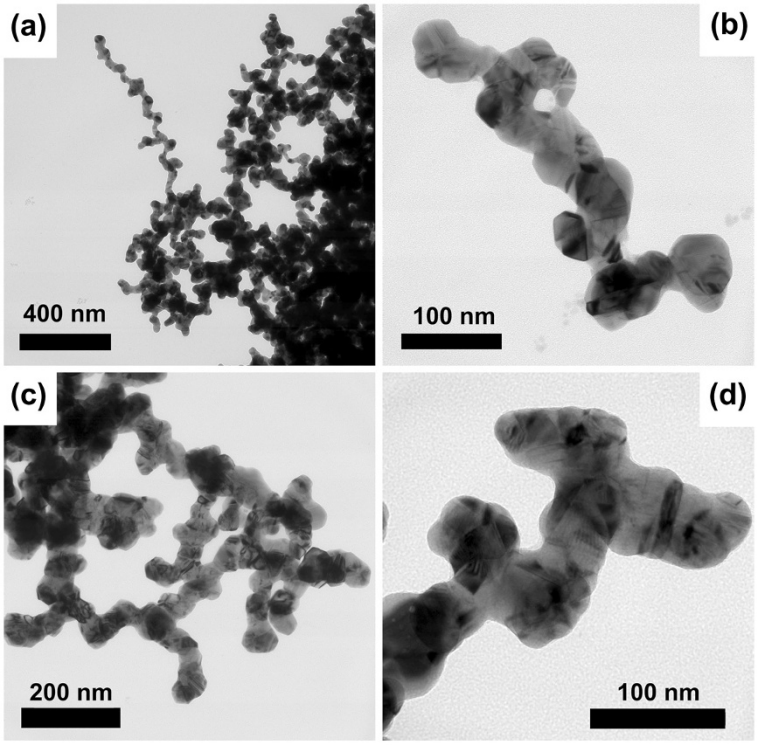

Figure 3 TEM images of the silver nanowires and nanomeshworks. (**a**) and (**b**) Typical branched silver nanowires. (**c**) Silver nanomeshworks. (**d**) High-resolution image of the nanomeshwork.

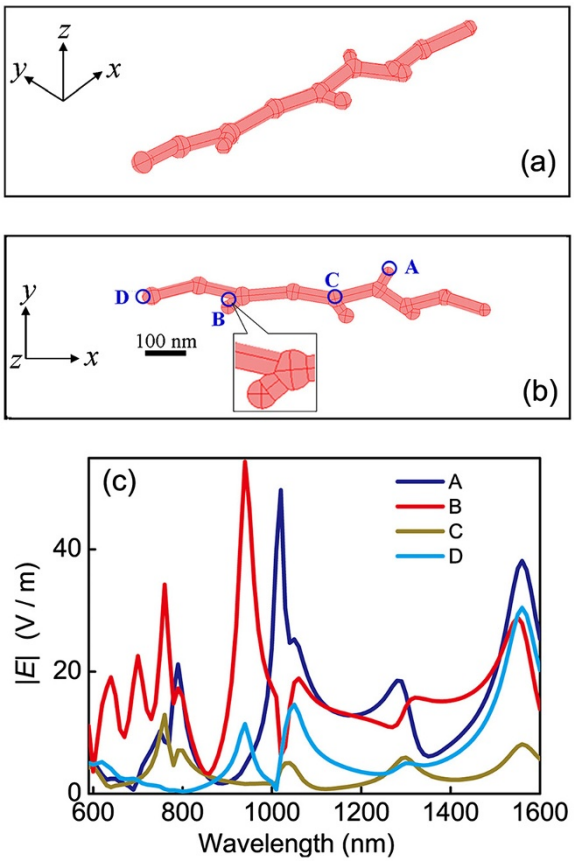

Figure 4 Simulation of the LSPR spectra at different positions distributed in a branched silver nanowire. (**a**) and (**b**) The geometry of the silver nanowire from the lateral view and the plane view, respectively. (**c**) The LSPR spectra at different positions highlighted in (**b**).

obviously with the increase of the exposure time. As the welded metal nanobranches and nanomeshworks increased, the color of the solution darkened rapidly with the extension of the exposure time, which is shown in the inset of Figure 1b. After a 5-h exposure procedure, the color of the solution turned to black which is obviously different from silver nanoparticles with regular shapes, such as bared nanowires [4] or nanoplates [3]. The optical spectra and the photographs of the solution are strong evidences to show that the ultimate silver nanostructures can trap light effectively in a broad wavelength range from the visible to the near-infrared wavelengths.

In the light exposure process, the small silver seeds aggregated and welded together when the solution was under exposure. The final morphology of the nanostructures depends on the concentrations of the capping agents, PVP, and L-arginine. As discussed in [18], high PVP concentration serves as a structure-directing agent to keep the nanostructure growth linear. High L-arginine concentration controls the reaction velocity and avoids the size growth of the nanoparticles [2]. Figure 3 shows the transmission electron microscopy (TEM) (Tecnai G2, FEI, Hillsboro, OR, USA) images of the ultimate silver nanostructures after exposure. The TEM samples were washed by ethanol and deionized water and then dispersed uniformly by ultrasonic before measurement. The typical nanostructures include branched nanowires and nanomeshworks. The diameter of these branched nanowires is about several tens of nanometers. Figure 3a,b shows linear branched nanowires with rough surfaces. It was found that there are many knobs and branches in the nanowires. Figure 3c shows nanomeshworks containing many short nanowires connected together randomly in three dimensions. From the high-resolution TEM image in Figure 3d, one can see that the branches

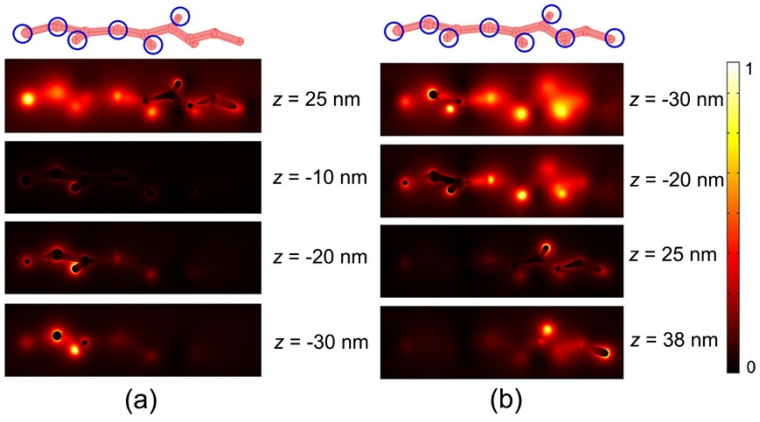

Figure 5 Simulation of the normalized electric-field |*E*| distributions. In the branched silver nanowire at different planes along the *z*-axis. The wavelength of the incident light is 940 and 1,020 nm in (**a**) and (**b**), respectively. The blue circles in the geometry images of the nanostructures illustrate the hot spots.

have joined together permanently, obviously different from the nanochains assembled by adjacent nanoparticles [17,19,20].

To investigate the light-trapping property of these nanostructures, we use three-dimensional FEM to simulate the electric field distribution of the branched nanostructures. Rectangular wave incoming from the upper x-y plane was set as the source boundary. The other outer boundaries were set as the scattering boundary condition. The cladding layer surrounding the silver nanostructures is water with a refractive index n = 1.33. The dispersion coefficient of water is neglected in the simulation. The dielectric constant of silver is taken from [29].

We first investigated the optical property of the branched silver nanowires. In the numerical model, we created a branched nanowire with randomly distributed branches and knobs referred to the morphology shown in the TEM images of Figure 3a,b. The configuration of the silver nanowire is shown in Figure 4a,b. The morphologic characteristics are listed as follows: the nanowire is knotty with an average diameter of 30 nm, the distance between the adjacent knobs is approximately 100 nm, the diameter of the knobs is between 30 and 50 nm, the branches connect to the bus nanowire with random angles, and the total length of the nanowire is approximately 800 nm. Figure 4c shows the relationship between the amplitude of the normalized electric field $|E|$ and the wavelength at different positions of the branched silver nanowire including the branch, the corner between two branches, the junction, and the end as labeled by A, B, C, and D, respectively, in Figure 4b. There are many resonance bands covering the wavelength range from the visible to the near-infrared wavelengths in the optical spectra. The bandwidths of the resonance bands are wide, and the amplitudes at the resonance peaks are high, especially at the branches and the corner area. Figure 5 shows the simulation results of the normalized electric field spatial distribution at different z positions seen from the x-y plane. The wavelength of the incident light is 940 and 1,020 nm in Figure 5a,b, respectively. Light can be easily localized at the positions of the knobs and the corners between the branches when it propagated along the nanowires with rough surfaces. It leads to various wavelength-dependent 'hot spots' [3,21] which are randomly distributed in the nanostructures. The light intensity at the area of the hot spots can be enhanced greatly, leading to a strong interaction of light with matters.

Figure 6 shows the LSPR spectra at different positions distributed in a silver nanomeshwork. The complicated meshwork is formed by randomly distributed short branches in three-dimensional space, as illustrated in Figure 6a,b. The diameter and the length of the short branches were set to be approximately 30 and 100 nm, respectively. In Figure 6c, the three curves represent the normalized electric field $|E|$ at the junction, the branch, and the end of the meshwork highlighted in Figure 6b. The LSPR spectra also exhibit multiple resonance bands with intense light enhancement in a wide wavelength range at the branch and the end area of the nanomeshwork, which

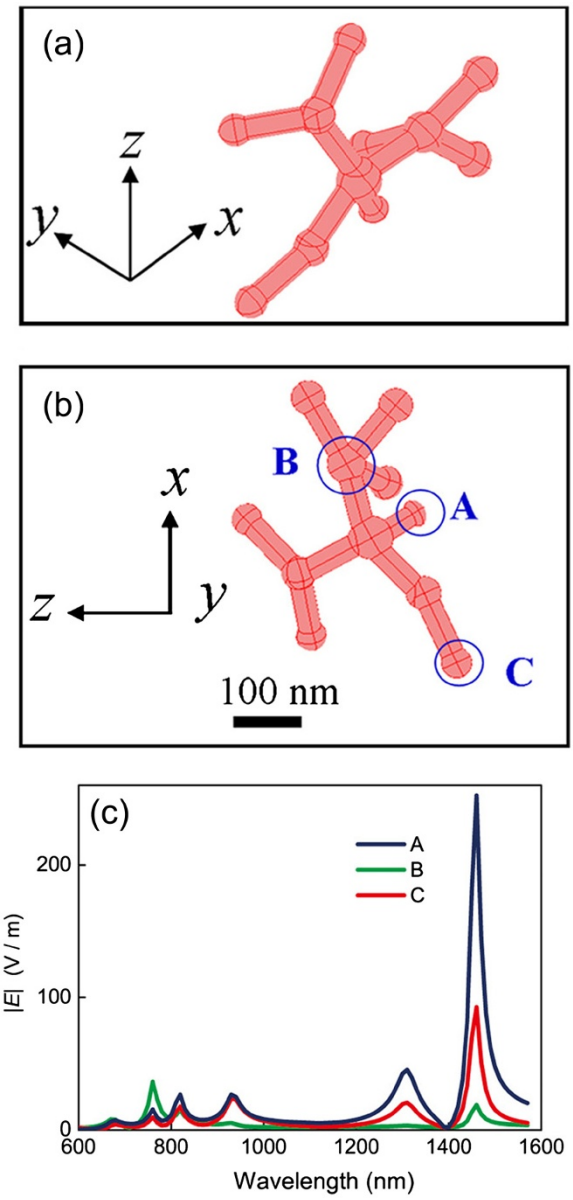

Figure 6 Simulation of the LSPR spectra at different positions distributed in a silver nanomeshwork. (**a**) and (**b**) The geometry of the silver nanomeshwork from the lateral view and the plane view, respectively. (**c**) The LSPR spectra at different positions highlighted in (**b**).

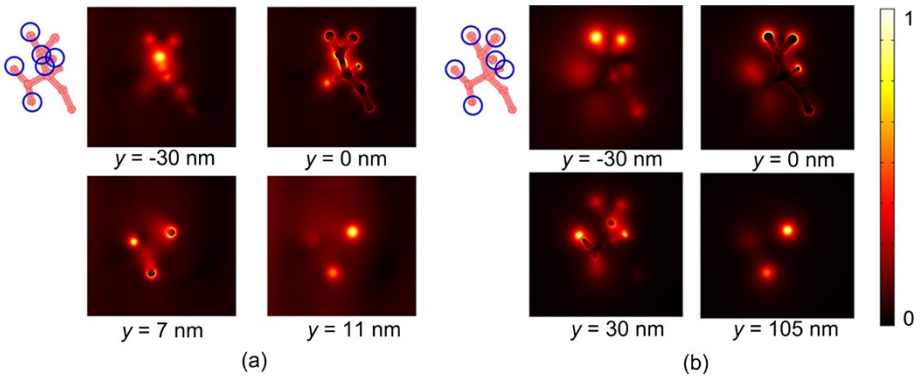

Figure 7 Simulation of the normalized electric-field |*E*| distributions. In the silver nanomeshwork at different planes along the *z*-axis. The wavelength of the incident light is 760 and 1,460 nm in (**a**) and (**b**), respectively. The blue circles in the geometry images of the nanostructures illustrate the hot spots.

is the same phenomenon as the nanowires. However, the light enhancement at the junction area is not obvious. It is because the longitudal resonant cavity length of the nanomeshwork is much shorter than that of the nanowire in our models. For such nanostructures with short resonant cavity length, light is easily be localized at the branches and the corner area rather than the middle area without sharp corners. Figure 7 shows the simulation results of the wavelength-dependent normalized electric field |*E*| distributions in the silver nanomeshwork at different planes along the *z*-axis. All images shown so far indicate that the silver nanomeshwork behaves like a three-dimentional 'light cage' which traps light at those randomly distributed branches and knobs. The distribution of the hot spots is also wavelength dependent. Such nanostructures can trap light with different wavelengths effectively in large-space areas.

The above simulation results indicate that such randomly constructed silver nanostructures with rough surfaces and multi-branches have high light-trapping efficiency, in accordance with the measured extinction spectra.

Conclusions

In this study, we introduce a simple chemical method for the fabrication of high-density branched silver nanostructures. Both experimental measurement and relative three-dimensional numerical simulation results show that these nanostructures have significant properties as follows: First, these branched silver nanostructures have significant light-trapping and scattering properties in a broad wavelength range. Second, light can propagate in a longer distance along the waveguide-like plasmonic nanostructures to improve the interaction between the surrounding materials and light. Third, the fabrication routes with easy operation and high yields meet the satisfaction of the large-scale production. These properties make such nanostructures useful in practice applications, such as photovoltaics, bio-chemical sensing, and optical processing.

Competing interests

The authors declare that they have no competing interests.

Authors' contributions

XYZ carried out the main part of synthetic, analytical, and simulation works and drafted the manuscript. SQZ, LDW, and YJS participated in the synthetic and analytical works. TZ, XFL, and QLW participated in the discussion of the experimental details and participated in the draft preparation. All authors read and approved the final manuscript.

Acknowledgments

This work is supported by NSFC under grant number 60977038, Doctoral Fund of Ministry of Education of China under grant number 20110092110016, the National Basic Research Program of China (973 Program) under grant number 2011CB302004, the Scientific Research Foundation of Graduate School of Southeast University under grant number YBPY1104, and the Foundation of Key Laboratory of Micro-Inertial Instrument and Advanced Navigation Technology, Ministry of Education, China.

Author details

[1]School of Electronic Science and Engineering, Southeast University, Nanjing 210096, People's Republic of China. [2]Key Laboratory of Micro-Inertial Instrument and Advanced Navigation Technology, Ministry of Education, Nanjing 210096, People's Republic of China. [3]Suzhou Key Laboratory of Metal Nano-Optoelectronic Technology, Suzhou Research Institute of Southeast University, Suzhou 215123, People's Republic of China. [4]Institute of Optics and Electronics, CAS, PO Box 350, Shuangliu, Chengdu 610209, China.

Received: 3 September 2012 Accepted: 21 October 2012
Published: 27 October 2012

References

1. Lu XM, Rycenga M, Skrabalak SE, Wiley B, Xia YN: **Chemical synthesis of novel plasmonic nanoparticles.** *Annu Rev Phys Chem* 2009, **60**:167–192.
2. Pietrobon B, Kitaev V: **Photochemical synthesis of monodisperse size-controlled silver decahedral nanoparticles and their remarkable optical properties.** *Chem Mater* 2008, **20**:5186–5190.
3. Zhang XY, Hu AM, Zhang T, Lei W, Xue XJ, Zhou YH, Duley WW: **Self-assembly of large-scale and ultrathin silver nanoplate films with tunable plasmon resonance properties.** *ACS Nano* 2011, **5**:9082–9092.

4. Peng P, Hu AM, Huang H, Gerlich AP, Zhao BX, Zhou YN: **Room-temperature pressureless bonding with silver nanowire paste: towards organic electronic and heat-sensitive functional devices packaging.** *J Mater Chem* 2012, **22:**12997–13001.
5. Peng P, Huang H, Hu AM, Gerlich AP, Zhou YN: **Functionalization of silver nanowire surfaces with copper oxide for surface-enhanced Raman spectroscopic bio-sensing.** *J Mater Chem* 2012, **22:**15495–15499.
6. Ditlbacher D, Hohenau A, Wagner D, Kreibig U, Rogers M, Hofer F, Aussenegg FR, Krenn JR: **Silver nanowires as surface plasmon resonators.** *Phys Rev Lett* 2005, **95:**257403.
7. Gu L, Sigle W, Koch CT, Ogüt B, van Aken PA, Talebi N, Vogelgesang R, Mu JL, Wen XG, Mao J: **Resonant wedge-plasmon modes in single-crystalline gold nanoplatelets.** *Phys. Rev. B* 2011, **83:**195433.
8. Hu A, Peng P, Alarifi H, Zhang XY, Guo JY, Zhou Y, Duley WW: **Femtosecond laser welded nanostructures and plasmonic devices.** *J Laser Appl* 2012, **24:**042001.
9. Zhang T, Zhang XY, Xue XJ, Wu XF, Li C, Hu A: **Plasmonic properties of welded metal nanoparticles.** *Open Surf Sci J* 2011, **3:**76–81.
10. Messina E, Cavallaro E, Cacciola A, Saija R, Borghese F, Denti P, Fazio B, Andrea CD, Gucciardi PG, Iati MA, Meneghetti M, Compagnini G, Amendola V, Maragò OM: **Manipulation and Raman spectroscopy with optically trapped metal nanoparticles obtained by pulsed laser ablation in liquids.** *J Phys Chem C* 2011, **115:**5115–5122.
11. Hu A, Guo JY, Alarifi H, Patane G, Zhou Y, Compagnini G, Xu CX: **Low temperature sintering of Ag nanoparticles for flexible electronics packaging.** *Appl Phys Lett* 2010, **97:**153117.
12. Magdassi S, Grouchko M, Berezin O, Kamyshny A: **Triggering the sintering of silver nanoparticles at room temperature.** *ACS Nano* 2010, **4:**1943–1948.
13. Liang CL, Zhong K, Liu M, Jiang L, Liu SK, Xing DD, Li HY, Na Y, Zhao WX, Tong YX, Liu P: **Synthesis of morphology-controlled silver nanostructures by electrodeposition.** *Nano-Micro Lett* 2010, **2:**6–10.
14. Masurkar SA, Chaudhari PR, Shidore VB, Kamble SP: **Rapid biosynthesis of silver nanoparticles using cymbopogan citratus (lemongrass) and its antimicrobial activity.** *Nano-Micro Lett* 2011, **3:**189–194.
15. Shrivastava S, Dash D: **Label-free colorimetric estimation of proteins using nanoparticles of silver.** *Nano-Micro Lett* 2010, **2:**164–168.
16. Angelescu DG, Vasilescu M, Somoghi R, Donescu D, Teodorescu VS: **Kinetics and optical properties of the silver nanoparticles in aqueous L64 block copolymer solutions.** *Colloids and Surfaces A: Physicochem Eng Aspects* 2010, **366:**155–162.
17. Polavarapu L, Xu QH: **Water-soluble conjugated polymer-induced self-assembly of gold nanoparticles and its application to SERS.** *Langmuir* 2008, **24:**10608–10611.
18. Zhang DF, Niu LY, Jiang L, Yin PG, Sun LD, Zhang H, Zhang R, Guo L, Yan CH: **Branched gold nanochains facilitated by polyvinylpyrrolidone and their SERS effects on p-aminothiophenol.** *J Phys Chem C* 2008, **112**:16011–16016.
19. Jia H, Bai XT, Li N, Yua L, Zheng LQ: **Siloxane surfactant induced self-assembly of gold nanoparticles and their application to SERS.** *Cryst EngComm* 2011, **13:**6179–6184.
20. Luo ZX, Yang WS, Peng AD, Ma Y, Fu HB, Yao JN: **Net-like assembly of Au nanoparticles as a highly active substrate for surface-enhanced Raman and infrared spectroscopy.** *J Phys Chem A* 2009, **113:**2467–2472.
21. Yang J, Wang ZY, Zong SF, Song CY, Zhang RH, Cui YP: **Distinguishing breast cancer cells using surface-enhanced Raman scattering.** *Anal Bioanal Chem* 2012, **402:**1093–1100.
22. Yang Y, Shi JL, Tanaka T, Nogami M: **Self-assembled silver nanochains for surface-enhanced Raman scattering.** *Langmuir* 2007, **23:**12042–12047.
23. Zhang XY, Zhang T, Hu A, Song YJ, Duley WW: **Controllable plasmonic antennas with ultra narrow bandwidth based on silver nano-flags.** *Appl Phys Lett* 2012, **101:**153118.
24. Garnett EC, Cai W, Cha JJ, Mahmood F, Connor ST, Christoforo MG, Cui Y, McGehee MD, Brongersma ML: **Self-limited plasmonic welding of silver nanowire junctions.** *Nat Mater* 2012, **11:**241–249.
25. Aatwater HA, Polman A: **Plasmonics for improved photovoltaic devices.** *Nat Mater* 2010, **9**:205–213.
26. Mak GY, Zhu L, Ma Z, Huang SY, Lam EY, Choi HW: **Plasmonically enhanced quantum-dot white-light InGaN light-emitting diode.** *J Phys D: Appl Phys* 2011, **44:**224016.
27. Zhang XY, Hu A, Zhang T, Xue XJ, Wen JZ, Duley WW: **Subwavelength plasmonic waveguides based on ZnO nanowires and nanotubes: a theoretical study of thermo-optical properties.** *Appl Phys Lett* 2010, **96:**043109.
28. Zhang XY, Hu A, Wen JZ, Zhang T, Xue XJ, Zhou Y, Duley WW: **Numerical analysis of deep sub-wavelength integrated plasmonic devices based on semiconductor-insulator-metal strip waveguides.** *Opt Express* 2010, **18:**18945–18959.
29. Rakić AD, Djurišić AB, Elazar JM, Majewski ML: **Optical properties of metallic films for vertical-cavity optoelectronic devices.** *Appl Opt* 1998, **37:**5271–5283.

doi:10.1186/1556-276X-7-596
Cite this article as: Zhang *et al.*: Fabrication and spectroscopic investigation of branched silver nanowires and nanomeshworks. *Nanoscale Research Letters* 2012 **7**:596.